Supplementary Discussion

Novel targets for Huntington's disease in an mTOR-independent autophagy pathway

Andrea Williams[1], Sovan Sarkar[1], Paul Cuddon[1], Evangelia K. Ttofi, Shinji Saiki, Farah H. Siddiqi, Luca Jahreiss, Angeleen Fleming, Dean Pask, Paul Goldsmith, Cahir J. O'Kane, R. Andres Floto and David C. Rubinsztein[2]

[1]*These authors contributed equally to this work*

[2]*Correspondence:* David C. Rubinsztein – E-mail: dcr1000@hermes.cam.ac.uk; Tel: (0)1223 762608; Fax: (0)1223 331206

Cell-type specificity

In this paper we have studied a range of cell types. However, the key pathways studied in this paper have all been validated in COS-7 cells, such as the link from cAMP-Epac to IP_3 (**Figs. 2b, 2e–h**), the effects of IP_3 on autophagy (previously demonstrated[1]) (**Fig. 2i)**, the Epac-PLC-ε to calpain link (**Fig. 3e** and **Supplementary Figs. 3k, l** online), the calpain effect (**Figs. 4f, g, 5e, f** and **Supplementary Figs. 4a, b, m, n** online), calpain cleavage of $G_{s\alpha}$ (**Supplementary Fig. 6a** online), elevation of cAMP levels by calpain and $G_{s\alpha}$ activation (**Supplementary Figs. 6d, e** online), the demonstration that cAMP can modulate calpain effects (**Fig. 6c**), and clarification that the pathway is mTOR-independent (**Figs 7a–f** and **Supplementary Figs. 6i, j** online). Furthermore, the key elements of the pathways and the drug effects have been validated in a range of cell types in cell models and *in vivo*, suggesting that these are not cell-type specific effects. While we can not exclude the possibility that there may be cell-type specific additional signals that contribute to these drug effects, the pathways studied are well-conserved. Of importance, the Epac pathway is well characterized in neurons[2-5] (**Supplementary Fig. 3f** online). Furthermore, $G_{s\alpha}$ and PLC-ε are expressed ubiquitously[6, 7], and the PLC-ε link with calpain activation is well recognized.

Intracytosolic Ca^{2+} and autophagy

Various studies have demonstrated raised intracytosolic Ca^{2+} levels and calpain activities in HD patients and animal models[8-11]. Thus, the pathway from Ca^{2+} to calpain to $G_{s\alpha}$ to cAMP to IP_3 is likely to be activated. IP_3 receptor activation (e.g., with PLC-ε overexpression) will lead to Ca^{2+} release and calpain activation (**Supplementary Fig. 3k** online). The autophagy-blocking effects of this activated

pathway will be reversed by the drugs we have identified (**Figs. 3a–e, 4g, 6c** and **Supplementary Figs. 3o, 4g–i, k** online). Direct calpain activation also blocks autophagy (**Figs. 4f** and **5e, f**). The PLC-ε effects appear to be directly mediated via calpain as they are blocked by calpeptin (**Fig. 3e**). However, it may be difficult to exclude other additional effectors of IP_3. While IP_3-receptor dependent Ca^{2+} release from the ER into the cytosol blocks autophagy via a calpain-dependent mechanism, one needs to ask whether the converse is mediated via the same process. In other words, if one decreases IP_3 levels, does this enhance autophagy by reducing the amount of ER-cytosol Ca^{2+} release? While it has been proposed that blocking IP_3 receptors increases autophagy in a manner that is independent of steady state Ca^{2+} levels[12], the alternative model may be difficult to prove as the Ca^{2+} levels may be at the limit of detection with such approaches or with PLC-ε inhibition. As all cells will show transient changes in intracytosolic Ca^{2+}, changes may be mediated via such oscillations (or transients) (which are affected by blocking the IP_3 receptor specific Ca^{2+} oscillatory activity[13, 14]), which may not give an obvious decrease in steady state intracellular Ca^{2+} levels. Such Ca^{2+} oscillations or transients (which are IP_3-dependent in neurons and can occur even in the absence of action potentials) can impact on calpain activity[15, 16]. The key experiment, which is very difficult to do, requires testing what proportion of the time the cells manifest transient increases of Ca^{2+} above the threshold levels in cells required to activate calpains in individual cells treated with IP_3 receptor blockers or IP_3 reducing agents. This may be impossible to assess in measurements of cell populations where transients are not synchronized, as is likely to be the case in the study of Criolla *et al*[12]. Also note that the latter level required for calpain activation in whole cells (as opposed to *in vitro)* is also elusive at present, largely precluding the experiment in practice. However, we cannot exclude

the possibility that distinct mechanisms operate with decreasing and increasing IP_3 levels or that more than one pathway of relevance to autophagy is affected (e.g., Ca^{2+}-dependent and Ca^{2+}-independent). Unfortunately, measurement of many of the key intermediates under such conditions is difficult and hampered by lack of assays sensitive to low levels of mediators like cAMP and calpain.

Recently, Hoyer-Hansen and colleagues reported that intracytosolic Ca^{2+} elevations enhance autophagy[17], contrasting with both our data and those of Seglen and colleagues[18]. However, the contradictory data are difficult to interpret conclusively for two reasons. First, while long-lived protein clearance was enhanced by agents that increase intracytosolic Ca^{2+}, this may have been due to calpain-mediated proteolysis, as no clearance data were shown in the presence of autophagy inhibitors[17]. Second, the major tool used to assess autophagy was steady state-levels of EGFP-LC3 vesicles. The specificity of their readout was difficult to interpret, particularly as high levels of these vesicles were observed with agents that increased intracytosolic Ca^{2+} even when 3-MA or siRNAs that prevent autophagosome formation were used[17]. Furthermore, no LC3-II or autophagosome flux data were presented. In an early paper, using a methodology similar to that of Seglen and co-workers, Grinde reported that verapamil blocks starvation-induced autophagy in rat hepatocytes[19]. It is conceivable that intracytosolic Ca^{2+} may have different effects on autophagy in starvation versus fed conditions. However, recent data from Yuan and colleagues support our findings that L-type Ca^{2+} channel inhibitors induce autophagy[20], although this study, like the Grinde study, have not sought to identify mediators of the Ca^{2+} effects. Our thapsigargin data (**Supplementary Figs. 4a–u** online) and the possible conflicting data in the literature suggest that the effects of certain drugs that perturb intracytosolic Ca^{2+} are likely to have complex effects on

autophagy and may even acts at different stages of the pathway. In the case of thapsigargin, the effects may be not due to changes in the cytosolic Ca^{2+} levels but due to depletion of the ER pool and ER stress effects. However, it is also possible that perturbations restricted to the intracytosolic Ca^{2+} pool may have complex effects.

Calpains and autophagy

A recent paper by Dermachi and colleagues that studied cells where the 28 kDa calpain regulatory subunit (calpain 4) was knocked out, suggested that calpain activity was essential for autophagy[21], and therefore appears to contradict our data. However, much of the data in their paper focused on autophagy after induction by other agents, like rapamycin, rather than basal autophagy. Actually, much of their data may correspond with ours. For instance, in normal medium, their cells with deficient calpain activity have more autophagosomes (LC3 puncta) and elevated levels of LC3-II[21]. We believe that the most important measure of autophagy is reflected by clearance rates of autophagy substrates – the autophagic flux. We have studied two different autophagy substrates in various conditions (including proteasome and autophagy inhibition). Demarchi and co-workers restricted their studies to analyses of long-lived protein clearance. In general, the majority of long-lived protein clearance is mediated by (macro)autophagy[22, 23]. Unfortunately, the way these studies were performed suggests that the bulk of the clearance that was analysed under their conditions was not by macroautophagy, as at least two-thirds of the clearance was 3-MA-independent[21]. Also, it appears that the clearance studies they showed were only performed in one line of control and calpain 4-deficient MEFs[21]. As such lines can drift (e.g., due to selection of cells with protective/compensatory mutations) and end up having certain characteristics that result in them being

unmatched for certain experiments. The key clearance data would have been more robust if tested in other ways (e.g., siRNA knockdown or replacing the calpain small subunit in the knockdown MEFs). Nevertheless, we cannot exclude the possibility that the loss of the calpain 4 subunit may truly abrogate autophagy. This may be reconcilable with our data; if minimal calpain activity is required for autophagy but if higher levels are inhibitory. Alternatively, calpain 4 may be necessary for autophagy via a calpain-activity-independent mechanism.

Supplementary Discussion References

1. Sarkar, S. *et al.* Lithium induces autophagy by inhibiting inositol monophosphatase. *J. Cell Biol.* **170**, 1101–1111 (2005).
2. Shi, G.X., Rehmann, H. & Andres, D.A. A novel cyclic AMP-dependent Epac-Rit signaling pathway contributes to PACAP38-mediated neuronal differentiation. *Mol. Cell Biol.* **26**, 9136–9147 (2006).
3. Ster, J. *et al.* Exchange protein activated by cAMP (Epac) mediates cAMP activation of p38 MAPK and modulation of Ca^{2+}-dependent K^{+} channels in cerebellar neurons. *Proc. Natl. Acad. Sci. USA* **104**, 2519–2524 (2007).
4. Enserink, J.M. *et al.* A novel Epac-specific cAMP analogue demonstrates independent regulation of Rap1 and ERK. *Nat. Cell Biol.* **4**, 901–906 (2002).
5. Schmidt, M. *et al.* A new phospholipase-C-calcium signalling pathway mediated by cyclic AMP and a Rap GTPase. *Nat. Cell Biol.* **3**, 1020–1024 (2001).
6. Weinstein, L.S., Xie, T., Zhang, Q.H. & Chen, M. Studies of the regulation and function of the Gs alpha gene Gnas using gene targeting technology. *Pharmacol. Ther.* **115**, 271–291 (2007).
7. Kelley, G.G., Reks, S.E., Ondrako, J.M. & Smrcka, A.V. Phospholipase C(epsilon): a novel Ras effector. *EMBO J.* **20**, 743–754 (2001).
8. Zeron, M.M. *et al.* Increased sensitivity to N-methyl-D-aspartate receptor-mediated excitotoxicity in a mouse model of Huntington's disease. *Neuron* **33**, 849–860 (2002).
9. Tang, T.S. *et al.* Huntingtin and huntingtin-associated protein 1 influence neuronal calcium signaling mediated by inositol-(1,4,5) triphosphate receptor type 1. *Neuron* **39**, 227–239 (2003).

10. Gafni, J. & Ellerby, L.M. Calpain activation in Huntington's disease. *J. Neurosci.* **22**, 4842–4849 (2002).

11. Gafni, J. *et al.* Inhibition of calpain cleavage of huntingtin reduces toxicity: accumulation of calpain/caspase fragments in the nucleus. *J. Biol. Chem.* **279**, 20211–20220 (2004).

12. Criollo, A. *et al.* Regulation of autophagy by the inositol trisphosphate receptor. *Cell Death Differ.* **14**, 1029–1039 (2007).

13. Malysz, J., Donnelly, G. & Huizinga, J.D. Regulation of slow wave frequency by IP(3)-sensitive calcium release in the murine small intestine. *Am. J. Physiol. Gastrointest. Liver Physiol.* **280**, G439–G448 (2001).

14. Jaimovich, E. *et al.* Xestospongin B, a competitive inhibitor of IP_3-mediated Ca^{2+} signalling in cultured rat myotubes, isolated myonuclei, and neuroblastoma (NG108-15) cells. *FEBS Lett.* **579**, 2051–2057 (2005).

15. Fujita, H., Nedachi, T. & Kanzaki, M. Accelerated de novo sarcomere assembly by electric pulse stimulation in C2C12 myotubes. *Exp. Cell Res.* **313**, 1853–1865 (2007).

16. Jasoni, C.L., Todman, M.G., Strumia, M.M. & Herbison, A.E. Cell type-specific expression of a genetically encoded calcium indicator reveals intrinsic calcium oscillations in adult gonadotropin-releasing hormone neurons. *J. Neurosci.* **27**, 860–867 (2007).

17. Hoyer-Hansen, M. *et al.* Control of Macroautophagy by Calcium, Calmodulin-Dependent Kinase Kinase-beta, and Bcl-2. *Mol. Cell* **25**, 193–205 (2007).

18. Gordon, P.B., Holen, I., Fosse, M., Rotnes, J.S. & Seglen, P.O. Dependence of hepatocytic autophagy on intracellularly sequestered calcium. *J. Biol. Chem.* **268**, 26107–26112 (1993).

19. Grinde, B. Role of Ca^{2+} for protein turnover in isolated rat hepatocytes. *Biochem. J.* **216**, 529–536 (1983).

20. Zhang, L. *et al.* Small molecule regulators of autophagy identified by an image-based high-throughput screen. *Proc. Natl. Acad. Sci. USA* **104**, 19023–19028 (2007).

21. Demarchi, F. *et al.* Calpain is required for macroautophagy in mammalian cells. *J. Cell Biol.* **175**, 595–605 (2006).

22. Cuervo, A.M., Stefanis, L., Fredenburg, R., Lansbury, P.T. & Sulzer, D. Impaired degradation of mutant alpha-synuclein by chaperone-mediated autophagy. *Science* **305**, 1292–1295 (2004).

23. Klionsky, D.J. & Ohsumi, Y. Vacuolar import of proteins and organelles from the cytoplasm. *Annu. Rev. Cell Dev. Biol.* **15**, 1–32 (1999).

Supplementary Information

Novel targets for Huntington's disease in an mTOR-independent autophagy pathway

Andrea Williams[1], Sovan Sarkar[1], Paul Cuddon[1], Evangelia K. Ttofi, Shinji Saiki, Farah H. Siddiqi, Luca Jahreiss, Angeleen Fleming, Dean Pask, Paul Goldsmith, Cahir J. O'Kane, R. Andres Floto and David C. Rubinsztein[2]

[1]*These authors contributed equally to this work*

[2]*Correspondence:* David C. Rubinsztein – E-mail: dcr1000@hermes.cam.ac.uk; Tel: (0)1223 762608; Fax: (0)1223 331206

Supplementary Materials and Methods

Plasmids

Huntington's Disease (HD) gene exon 1 fragment with 74 polyQ repeats in pEGFP-C1 (Clontech) (EGFP-HDQ74) was described and characterised previously[1]. EGFP-LC3 and myc-LC3 constructs[2] (kind gifts from T. Yoshimori), wild-type phospholipase C epsilon construct[3] (kind gift from J. Lomasney), dominant-negative Rap2B S17N construct[4] (kind gift from Jean de Gunzburg), EGFP-Atg5[5], wild-type and K130R Atg5 constructs[6] (kind gifts from N. Mizushima), constitutive active S50E human m-calpain construct[7] (kind gift from A. Wells), rheb construct[8] (kind gift from K. L. Guan), cytosolic dsRed2-IP_3 kinase A (N-terminal 66 amino acids deleted) construct[9] (kind gift from R. Irvine), human LC3B construct (kind gift from M. Mizuguchi), GFP-lgp20 (kind gift from P. Luzio) and mCherry (kind gift from R. Tsien) were obtained. pcDNA3.1 construct was used as an empty vector.

Human LC3B was subcloned from pGEX-6P-1 into pcDNA3 (Invitrogen) using BamHI and EcoRI (both NEB). mCherry was amplified by PCR with the following primers: 5'-TA CCG AGC TCG GTA CCC GCC ACC AT-3' and 3'-G CTG TAC AAG CAA GGA TCC TGC-5'. The resulting fragments were purified (Qiagen gel extraction kit), digested with KpnI and EcoRI (both NEB) and subcloned in frame into the 5' end of hLC3B pcDNA3.

Compounds

Cells were treated with various compounds for various time-points as stated under different experimental conditions including 0.3 μM/1 μM/3 μM verapamil hydrochloride, 1 μM loperamide hydrochloride, 1 μM nimodipine, 1 μM nitrendipine, 1 μM amiodarone hydrochloride, 0.3 μM/1 μM/3 μM clonidine hydrochloride, 0.3

μM/1 μM/3 μM rilmenidine, 1 μM (±)-Bay K8644, 1 μM KT5720, 1 μM minoxidil, 1 μM (R)-(+)-Bay K 8644 (**32**), 1 μM (S)-(-)-Bay K 8644 (**33**), 10 μM FPL64176, 10 μM tolazamide, 10 μM quinine sulphate, 10 μM rolipram, 200 μM NF449, 2.5 μM thapsigargin, 0.2 μM rapamycin, 400 nM bafilomycin A1 and 10 μM lactacystin (**34**) (all from Sigma); 10 μM/15 μM/20 μM/30 μM calpastatin, 50 μM ALLM (**35**), 50 μM calpeptin, 20 μM caspase inhibitor I (Z-VAD-FMK) (**36**), 10 μM ionomycin (**37**), 24 μM Forskolin, 100 nM/1000 nM PACAP 38 Ovine and 500 μM 2'5'dideoxyadenosine (2'5'ddA) (all from Calbiochem); 1 μM/10 μM N^6Benzoyl-cAMP (6-Bnz-cAMP), 1 μM/10 μM 8-(4-Chlorophenylthio)-2'-0-methyl-cAMP (8-CPT-2-Me-cAMP) and 1 mM N^6,2-O-Dibutyryl-cAMP (db-cAMP) (all from Biolog). Compounds were used at concentrations previously described as having the desired and expected effects on the targets described in this study effects in cell culture.

Mammalian cell lines, culture and transfection

African green monkey kidney cells (COS-7), human neuroblastoma cells (SK-N-SH), human cervical carcinoma cells (HeLa), HeLa cells stably expressing EGFP-LC3[10] (kind gift from A. M. Tolkovsky), Atg5 wild-type and knock-out mouse embryonic fibroblasts[6] (MEFs) (kind gifts from N. Mizushima) and normal rat kidney cells (NRK) were maintained in Dulbecco's Modified Eagle Medium (DMEM, Sigma) supplemented with 10% Fetal Bovine Serum (FBS, Sigma), 100 U/ml Penicillin/Streptomycin and 2 mM L-Glutamine (Sigma) at 37°C, 5 % Carbon dioxide (CO_2). Cells were plated in six-well dishes at a density of 1×10^5 cells per well for 24 h and transfected with pEGFP-HDQ74 (1.5 μg/well of 6-wells plate) using LipofectAMINE reagent for COS-7 cells and LipofectAMINE PLUS reagent for SK-N-SH cells using manufacturer's protocol (Invitrogen). The transfection mixture was

replaced after 4 h incubation at 37°C by various compounds. Transfected cells were fixed with 4% paraformaldehyde (Sigma) after 48h and mounted in 4',6-diamidino-2-phenylindole (DAPI, 3 mg/ml, Sigma) over coverslips on glass slides and analysed for aggregation and cell death. For immunoblotting, COS-7 cells were plated at a density of 3×10^5 cells per well and treated for 24 h. HeLa cells stably expressing Ub^{G76V}-GFP reporter[11] (kind gift from N.P. Dantuma) were grown in the same media used for COS-7 cells supplemented with 0.5 mg/ml G418.

Inducible PC12 stable cell lines expressing EGFP-tagged exon 1 of HD gene (EGFP-HDQ74)[12] and HA-tagged A53T α-synuclein mutant[13], previously characterised, were maintained at 75 μg/ml hygromycin B (Calbiochem) in standard DMEM with 10% horse serum (Sigma), 5% FBS, 100 U/ml penicillin/streptomycin, 2 mM L-glutamine, and 100 μg/ml G418 (GIBCO) at 37°C, 10% CO_2.

Quantification and analysis of aggregate formation and cell death

Approximately 200 EGFP-positive cells per sample were counted for the proportion of cells with green fluorescent EGFP-HDQ74 aggregates, as described previously[1, 14, 15]. If an EGFP-positive cell has one or many aggregates, the aggregate score is 'one'. If an EGFP-positive cell does not have any aggregate, the aggregate score is 'zero'. For example, the statement 'calpastatin significantly reduced EGFP-HDQ74 aggregates' means that calpastatin significantly reduced the proportion of EGFP-positive cells with EGFP-HDQ74 aggregates. Only EGFP-positive cells were counted so that we count only the transfected cells. Nuclei were stained with DAPI and those showing apoptotic morphology (fragmentation or pyknosis) were considered abnormal. These criteria are specific for cell death, which highly correlate with propidium iodide staining in live cells[16]. Analysis was performed using Nikon Eclipse

E600 fluorescence microscope (plan-apo 60x/1.4 oil immersion lens at room temperature) with observer blinded to identity of slides. Slides were coded and the code was broken after completion of experiment. All experiments were done in triplicate at least twice.

Assessment of autophagy by LC3

When autophagy is induced, the microtubule-associated protein 1 light chain 3 (LC3) is processed post-translationally into LC3-I, and then to LC3-II, which associates with autophagosome membranes[2]. Quantification of the number of cells with LC3-positive vesicles or LC3-II levels (versus actin) allows for a specific and sensitive assessment of autophagosome number in large numbers of cells[17].

Furthermore, as EGFP-LC3 overexpression does not affect autophagic activity, the numbers of EGFP-LC3 vesicles have frequently been used to assess autophagosome number[18]. For analysing the cells with EGFP-LC3 vesicles, we considered an EGFP-positive cell as having a score of 'zero' if there were 5 or fewer vesicles (as cells have basal levels of autophagy) and cells scored 'one' if they had >5 LC3-positive vesicles[14]. Analysis was performed using Nikon Eclipse E600 fluorescence microscope (plan-apo 60x/1.4 oil immersion lens at room temperature) with observer blinded to identity of slides. Slides were coded and the code was broken after completion of experiment. All experiments were done in triplicate at least twice.

Analysis of autophagosome-lysosome fusion

NRK cells were transfected 24 h after seeding, with 1 μg mCherry-LC3, 0.5 μg GFP-lgp120 per cover slip for 4 h in Optimem. They were then washed once in full medium and cultured in full medium with DMSO, 400 nM bafilomycin A1 or 2.5 μM

Thapsigargin for 24 h. Cells were fixed for 10 min in 4% PFA and mounted in Prolong Gold anti-fading solution (Invitrogen) containing DAPI (3 μg/ml). Cover slips were then blinded and 20 cells per treatment were imaged on a Zeiss Axiovert 200M microscope with a LSM 510 confocal attachment using a 63x 1.4 NA Plan Apochromat oil-immersion lens. Laser lines at 488 nm (GFP-lgp120) and 543 nm (mCherry-LC3) were used. These cells were then analysed in Zeiss LSM Image Browser 3.5 as follows: First, after switching off the GFP-channel, all mCherry-LC3 positive vesicles were counted and marked. Then the GFP-channel was switched back on and the number of double-labelled vesicles was counted. From these values the fraction of double-labelled vesicles was determined, i.e., the percentage of LC3-positive vesicles labelled with lgp120 was calculated.

We have confirmed that the expression of fluorescently-tagged LC3 in the cells does not result in aggregation, and the vesicles labelled with tagged-LC3 are virtually abolished with 3-methyladenine (3-MA) (**38**) treatment[19].

Immunocytochemistry

COS-7 cells were fixed with 4 % paraformaldehyde. Primary antibodies included anti-LC3 (kind gift from T. Yoshimori) and anti-cAMP (Chemicon). Standard fluorescence methods were used for detection and secondary antibodies used were goat anti-rabbit Alexa 488 Green and Alexa 594 Red (Cambridge Biosciences). Images were acquired on a Zeiss LSM510 META confocal microscope (63x 1.4NA plan-apochromat oil immersion) at room temperature using Zeiss LSM510 v3.2 software (Carl Zeiss, Inc.), and Adobe Photoshop 6.0 (Adobe Systems, Inc.) was used for subsequent image processing.

Western Blot Analysis

Cell pellets were lysed on ice in Laemmli buffer (62.5 mM Tris-HCl pH 6.8, 5 % β-mercaptoethanol, 10 % glycerol, and 0.01 % bromophenol blue) for 30 min in the presence of protease inhibitors (Roche Diagnostics). Samples were subjected to SDS–polyacrylamide gel electrophoresis and proteins were transferred to nitrocellulose membranes (Amersham Pharmacia Biotech). Primary antibodies used include anti-EGFP (8362-1, Clontech), anti-HA (12CA5, Covance), anti-mTOR (2972), anti-Phospho-mTOR (Ser2448) (2971), anti-p70 S6 Kinase (9202), anti Phospho-p70 S6 Kinase (Thr389) (9206), anti-4E-BP1 (9452), anti-Phospho-4E-BP1 (Thr37/46) (9459), all from Cell Signaling Technology, anti-calpain small subunit (μ- or m-calpain) (MAB3083, Chemicon), anti-calpain 1 (MAB3104, Chemicon), anti-calpain 2 domain III (208755, Calbiochem), anti-$G_{s\alpha}$ (06-237, Upstate), anti-LC3 (NB100-2220, Novus), anti-LC3 (kind gift from T. Yoshimori), anti-actin (A2066, Sigma) and anti-tubulin (Clone DM 1A, Sigma). Blots were probed with anti-mouse or anti-rabbit IgG-HRP (Amersham) and visualised using ECL or ECL Plus detection kit (Amersham).

Measurement of stored intracellular Ca^{2+}

Following 24 h treatment with 2.5 μM thapsigargin alone or in combination with 10 μM calpastatin or 50 μM ALLM (as previously described), COS-7 cells were pre-incubated with 1 μM Fura2-AM and an equal volume of Pluronic F127 (both Molecular Probes) for 45 min at room temperature in HEPES-buffered saline (HBS) containing 2 mM $CaCl_2$ and stored on ice. Aliquots of cells (~$5x10^5$ /run) were resuspended in nominally Ca^{2+}-free HBS. Stored intracellular Ca^{2+} was released into cytoplasm by adding 10 μM ionomycin. Experiments on PC12 cells were carried out

following a similar loading regime for cells (but using 4 μM Fura-2-AM) and were performed using HBS containing 2 mM Ca^{2+} as extracellular solution. All experiments were performed at 37°C and quantification of intracellular Ca^{2+} was achieved by monitoring Fura-2 fluorescence using a Cairn Spectrophotometer as described previously[20].

RNA Interference

*SMART*pool siRNA (pool of four different siRNA duplexes) against calpain 1 and calpain 2 and against GNAS (Dharmacon) were used for knockdown of the respective calpains and $G_{s\alpha}$. Control siRNA (Ambion) or si*GLO* RISC-free siRNA (Dharmacon), which is fluorescent and does not target any human or mouse genes, was used as a control. HeLa cells were transfected with siRNAs (200 nM per well) for 96 h using Oligofectamine (Invitrogen) according to manufacturer's protocol. For experiment with EGFP-LC3, HeLa cells were transfected with si*GLO* alone or in combination with calpain 1 siRNA or calpain 2 siRNA (total 320 nM per well in 1:3 ratio) for 96 h followed by transfection with EGFP-LC3 (1 μg per well) using LipofectAMINE PLUS (Invitrogen) for 4 h. Cells were fixed after 2 h and analysed by fluorescence microscopy. For experiment with EGFP-HDQ74, HeLa cells were transfected with EGFP-HDQ74 (1.5 μg per well) along with si*GLO* or control siRNA in presence or absence of calpain 1 siRNA, calpain 2 or GNAS siRNA (1:3 ratio as above) for 96 h using LipofectAMINE 2000 (Invitrogen) according to manufacturer's protocol. Cells were fixed after transfection and analysed by fluorescence microscopy. The total amount of siRNA in the above experiments is identical in control and calpain/$G_{s\alpha}$ knockdown cells.

Assay for cAMP levels

Cells were subjected to immunocytochemistry (described above) using rabbit anti-cAMP primary antibody (1:4000) (Chemicon) overnight and goat anti-rabbit Alexa 488 Green secondary antibody (1:1000) (Cambridge Biosciences) for 1 h. Images of the samples were acquired on a Zeiss LSM510 META confocal microscope (63x 1.4NA plan-apochromat oil immersion) at room temperature using Zeiss LSM510 v3.2 software (Carl Zeiss, Inc.), ensuring that the gain and the off-set were identical for all the samples. Analysis was performed by selecting individual mCherry (red)-positive cells and the mean green fluorescent intensity (arbitrary units) of cAMP was determined from 20 cells per slide from triplicate sample. Unpaired *t*-tests were performed on the means from each triplicate sample.

Rap2B activation assay

PC12 cells were plated into 9 cm dishes at a density of $3x10^5$ and treated with 24 μM Forskolin (Sigma) or DMSO (control) for 30 min. Cells were then washed in ice-cold PBS twice and lysed on ice for 10 min in 1x RIPA buffer (50 mM Tris HCl pH 7.4, 200 mM NaCl, 2.5 mM MgCl2, 1% NP40, 10% glycerol and complete protease inhibitors). Prior to lysis, the GST-RalGDS-RBD protein was first diluted 1:100 in RIPA buffer and then immobilised to GST-magnetic beads (Novagen) for 2 h under constant tumbling (5 μg protein to 15 μl of GST-magnetic bead). The lysate was then added to the protein-bound beads and the mixture was incubated for a further 45 min at 4^0C. Finally the mixture was washed four times with RIPA buffer, boiled with 40μl of 2x Laemmli buffer for 1 min to separate the beads from the protein complex and resolved by gel electrophoresis using anti-Rap2B.

Electron microscopy

Electron microscopy (EM) analysis of autophagosomes was performed using criteria as described previously[21].

***Drosophila* analysis**

Fly culture and crosses were carried out at 25°C and at 70% humidity, using Instant Fly Food (Philip Harris, Ashby de la Zouch, UK) unless otherwise stated. Flies were raised with a 12 h light: 12 h dark cycle. Aliquots of 0.5 M verapamil hydrochloride (Sigma, Poole, UK) in DMSO, or DMSO alone were added to the water that was used to prepare the instant fly food.

Virgin female flies of the genotype *y w; gmr-httNterm(1-171)Q120* (*gmrQ120)*[22] were allowed to mate with male flies from an isogenised w^{1118} stock[23] in food vials for 48 h. Flies were then transferred to vials containing instant fly food containing either drug in DMSO or DMSO alone. Progeny were collected 0-4 h after eclosion, kept on food of the same composition as they had been reared on, and scored for photoreceptor degeneration using the pseudopupil technique[24] two days after eclosion.

We previously analysed toluidine blue-stained plastic sections of *gmr-httQ120 Drosophila* eyes and characterized the rhabdomere loss in detail[25]. Consistent with a previous report[22], we observed loss of rhabdomeres followed by degeneration of the eyes, which manifested as structural disorganization but resulted in only subtle and low levels of photoreceptor loss[25]. We saw no loss of rhabdomeres in either wild-type flies, or transgenic flies expressing otherwise identical huntingtin transgenes with 23 glutamines. Since we observed some variability in the eye disorganization in Q120 flies and since it is difficult to quantify structural changes, we used the pseudopupil

technique as a quantifiable read-out. Loss of visible rhabdomeres in this model preceded photoreceptor death/loss assessed by toludine-blue staining of plastic sections and is a progressive degenerative phenotype seen only in flies expressing the mutant transgene (but not the wild-type transgene) and was not present at eclosion[22] (data not shown).

For pseudopupil analysis, heads were removed from adult male flies and mounted on microscope slides using nail polish. The ommatidia were analyzed using a 100x objective and bright field optics with bright illumination, with the observer blinded to the identity of the flies. Rhabdomere counts were carried out by analyzing 15 ommatidia per fly with around 20 flies per experiment for each treatment. In each experiment, we analysed flies from at least three different vials. The experiment was repeated on at least three independent occasions. Raw data from individual ommatidia from all experiments pooled were analyzed nonparametrically using a Mann-Whitney U test to determine significance levels, with the STATVIEW software, version 4.53 (Abacus Concepts). A paired Student's *t*-test was used to compare the experiment-average scores for each treatment.

Zebrafish analysis

Fish stocks and embryo microinjection. Rearing, breeding and staging of zebrafish (*Danio rerio*) were performed as described by[26]. Wild-type zebrafish were in-crossed descendants of the TL strain (Sheffield University, UK). Zebrafish were treated in accordance with Home Office Guidelines. EGFP, EGFP-HDQ23 and EGFP-HDQ71 constructs were cloned downstream of the zebrafish rhodopsin promoter[27] into a modified pEX100T vector (LTG, Promochem, ATCC 87436). EGFP-HDQ23 and EGFP-HDQ71 constructs are huntingin exon 1 wild-type and mutant fragments with

N-terminal EGFP tags, respectively, analogous to those used in cell culture experiments. Circular DNA was co-injected with IsceI meganuclease into one-cell stage embryos. Multiple founders were identified for each transgene.

Compound treatment. Zebrafish embryos were raised in 0.1 mM 1-phenyl-2-thiourea (PTU) from day 1 to day 3 post-fertilisation (d.p.f.) to inhibit pigment formation and screened for transgene expression using EGFP fluorescence. From 3 d.p.f. to 9 d.p.f., zebrafish were dark-reared in 0.1% DMSO, 100 μM 2'5'ddA, 3 μM verapamil, 3 μM clonidine, 1 μM calpastatin or 1 μM (±)-BayK8644 (all in E3 embryo medium – 5 mM NaCl, 0.17 mM KCl, 0.33 mM $CaCl_2$, 0.33 mM $MgSO_4$, 10-5% Methylene Blue pH 7.2), with drugs refreshed daily. Larvae were sacrificed under dim red light illumination and fixed with 4% PFA in PBS for the analysis of aggregates, or lysed in 80% RIPA, 100 mM DTT (both Sigma) and 10% protease inhibitor (Roche) for Western blotting.

Aggregate analysis. PFA was washed with PBS, followed by the addition of 30% sucrose for 1 h. Fish were then embedded into OCT medium, frozen on dry-ice, and sectioned at 12 μm intervals using a Cryostat. Sections were mounted in 80% glycerol in PBS. Aggregates were counted over 96 μm of the central eye, either side of the optic nerve, and means were calculated from 10 fish for each group. Data are compared using ANOVA and Dunnetts post-hoc T-test.

Western Blotting. Following an hour of lysis on ice, protein samples were diluted in sample buffer and boiled. Proteins were resolved on a 10% SDS-PAGE gel and blotted according to standard procedure. Membranes were blocked using SuperBlock (Pierce), and probed with a mouse monoclonal anti-rhodopsin antibody (1:1000 anti-Zpr3, ZFIN); mouse monoclonal anti-double cone antibody (anti-Zpr1, 1:2000, ZFIN) and rabbit polyclonal anti-EGFP antibody (1:20,000, Abcam). Membranes were

washed with TBS-T and probed with 1:10,000 anti-mouse and 1:20,000 anti-rabbit antibodies (Dako). After several washes with TBST, membranes were incubated with ECL reagent and exposed to Hyperfilm (both Amersham). Quantitative densitometry on rhodopsin expression was performed using ImageJ (NIH, US). Three independent experiments were performed for each treatment, each of which included 15 fish. Expression levels were compared using Student's *t*-test, relative to 71Q control.

Supplementary Information References

1. Narain, Y., Wyttenbach, A., Rankin, J., Furlong, R.A. & Rubinsztein, D.C. A molecular investigation of true dominance in Huntington's disease. *J. Med. Genet.* **36**, 739–746 (1999).
2. Kabeya, Y. *et al.* LC3, a mammalian homologue of yeast Apg8p, is localized in autophagosome membranes after processing. *EMBO J.* **19**, 5720–5728 (2000).
3. Lopez, I., Mak, E.C., Ding, J., Hamm, H.E. & Lomasney, J.W. A novel bifunctional phospholipase c that is regulated by Galpha 12 and stimulates the Ras/mitogen-activated protein kinase pathway. *J. Biol. Chem.* **276**, 2758–2765 (2001).
4. Lerosey, I., Chardin, P., de Gunzburg, J. & Tavitian, A. The product of the rap2 gene, member of the ras superfamily. Biochemical characterization and site-directed mutagenesis. *J. Biol. Chem.* **266**, 4315–4321 (1991).
5. Pyo, J.O. *et al.* Essential roles of Atg5 and FADD in autophagic cell death: dissection of autophagic cell death into vacuole formation and cell death. *J. Biol. Chem.* **280**, 20722–20729 (2005).
6. Mizushima, N. *et al.* Dissection of autophagosome formation using Apg5-deficient mouse embryonic stem cells. *J. Cell Biol.* **152**, 657–668 (2001).
7. Glading, A. *et al.* Epidermal growth factor activates m-calpain (calpain II), at least in part, by extracellular signal-regulated kinase-mediated phosphorylation. *Mol. Cell Biol.* **24**, 2499–2512 (2004).
8. Manning, B.D. & Cantley, L.C. Rheb fills a GAP between TSC and TOR. *Trends Biochem. Sci.* **28**, 573–576 (2003).

9. Schell, M.J., Erneux, C. & Irvine, R.F. Inositol 1,4,5-trisphosphate 3-kinase A associates with F-actin and dendritic spines via its N terminus. *J. Biol. Chem.* **276**, 37537–37546 (2001).

10. Bampton, E.T.W., Goemans, C.G., Niranjan, D., Mizushima, N. & Tolkovsky, A.M. The dynamics of autophagy visualised in live cells: from autophagosome formation to fusion with endo/lysosomes. *Autophagy* **1**, 23–36 (2005).

11. Dantuma, N.P., Lindsten, K., Glas, R., Jellne, M. & Masucci, M.G. Short-lived green fluorescent proteins for quantifying ubiquitin/proteasome-dependent proteolysis in living cells. *Nat. Biotechnol.* **18**, 538–543 (2000).

12. Wyttenbach, A. *et al.* Polyglutamine expansions cause decreased CRE-mediated transcription and early gene expression changes prior to cell death in an inducible cell model of Huntington's disease. *Hum. Mol. Genet.* **10**, 1829–1845 (2001).

13. Webb, J.L., Ravikumar, B., Atkins, J., Skepper, J.N. & Rubinsztein, D.C. Alpha-Synuclein is degraded by both autophagy and the proteasome. *J. Biol. Chem.* **278**, 25009–25013 (2003).

14. Sarkar, S. *et al.* Lithium induces autophagy by inhibiting inositol monophosphatase. *J. Cell Biol.* **170**, 1101–1111 (2005).

15. Ravikumar, B., Duden, R. & Rubinsztein, D.C. Aggregate-prone proteins with polyglutamine and polyalanine expansions are degraded by autophagy. *Hum. Mol. Genet.* **11**, 1107–1117 (2002).

16. Wyttenbach, A. *et al.* Heat shock protein 27 prevents cellular polyglutamine toxicity and suppresses the increase of reactive oxygen species caused by huntingtin. *Hum. Mol. Genet.* **11**, 1137–1151 (2002).

17. Mizushima, N. Methods for monitoring autophagy. *Int. J. Biochem. Cell Biol.* **36**, 2491–2502 (2004).

18. Mizushima, N., Yamamoto, A., Matsui, M., Yoshimori, T. & Ohsumi, Y. In vivo analysis of autophagy in response to nutrient starvation using transgenic mice expressing a fluorescent autophagosome marker. *Mol. Biol. Cell* **15**, 1101–1111 (2004).

19. Jahreiss, L., Menzies, F.M. & Rubinsztein, D.C. The itinerary of autophagosomes: From peripheral formation to kiss-and-run fusion with lysosomes. *Traffic* (2008).

20. Floto, R.A. *et al.* Loss of function of a lupus-associated FcgammaRIIb polymorphism through exclusion from lipid rafts. *Nat. Med.* **11**, 1056–1058 (2005).

21. Pattingre, S. *et al.* Bcl-2 antiapoptotic proteins inhibit Beclin 1-dependent autophagy. *Cell* **122**, 927–939 (2005).

22. Jackson, G.R. *et al.* Polyglutamine-expanded human huntingtin transgenes induce degeneration of *Drosophila* photoreceptor neurons. *Neuron* **21**, 633–642 (1998).

23. Ryder, E. *et al.* The DrosDel collection: a set of P-element insertions for generating custom chromosomal aberrations in *Drosophila melanogaster*. *Genetics* **167**, 797–813 (2004).

24. Franceschini, N. in *Information processing in the visual system of Drosophila* (ed. Wehner, R.) 75–82 (Springer, Berlin, 1972).

25. Berger, Z. *et al.* Rapamycin alleviates toxicity of different aggregate-prone proteins. *Hum. Mol. Genet.* **15**, 433–442 (2006).

26. Kimmel, C.B., Ballard, W.W., Kimmel, S.R., Ullmann, B. & Schilling, T.F. Stages of embryonic development of the zebrafish. *Dev. Dyn.* **203**, 253–310 (1995).

27. Kennedy, B.N., Vihtelic, T.S., Checkley, L., Vaughan, K.T. & Hyde, D.R. Isolation of a zebrafish rod opsin promoter to generate a transgenic zebrafish line expressing enhanced green fluorescent protein in rod photoreceptors. *J. Biol. Chem.* **276**, 14037–14043 (2001).

28. Gafni, J. & Ellerby, L.M. Calpain activation in Huntington's disease. *J. Neurosci.* **22**, 4842–4849 (2002).

29. Sato-Kusubata, K., Yajima, Y. & Kawashima, S. Persistent activation of Gsalpha through limited proteolysis by calpain. *Biochem. J.* **347**, 733–740 (2000).

30. Sarkar, S., Davies, J.E., Huang, Z., Tunnacliffe, A. & Rubinsztein, D.C. Trehalose, a novel mTOR-independent autophagy enhancer,accelerates the clearance of mutant huntingtin and alpha-synuclein. *J. Biol. Chem.* **282**, 5641–5652 (2007).

31. Rubinsztein, D.C. The roles of intracellular protein-degradation pathways in neurodegeneration. *Nature* **443**, 780–786 (2006).

Supplementary Figure 1

a

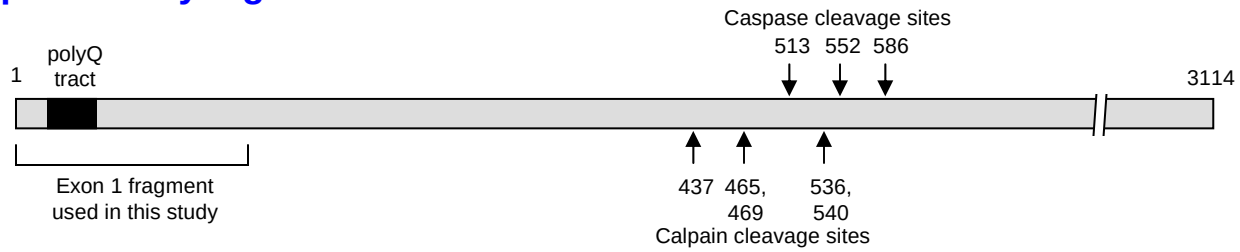

b **List of screen hits and various compounds used in this study that modulate the clearance of aggregate-prone proteins by autophagy.**

Compound	Action	Effect on clearance of aggregate-prone proteins
(±) Verapamil hydrocloride	L-type Ca^{2+} channel antagonist	Increase
Loperamide hydrocloride	L-type Ca^{2+} channel antagonist	Increase
Nimodipine	L-type Ca^{2+} channel antagonist	Increase
Amiodarone hydrochloride	L-type Ca^{2+} channel antagonist	Increase
Nitrendipine	L-type Ca^{2+} channel antagonist	Increase
(±)-Bay K8644	L-type Ca^{2+} channel agonist	Decrease
(R)-(+)-Bay K8644	L-type Ca^{2+} channel antagonist	Increase
(S)-(-)-Bay K8644	L-type Ca^{2+} channel agonist	Decrease
Minoxidil	ATP-K^+ channel activator	Increase
Clonidine hydrochloride	α2A adrenergic receptor antagonist/ imidazoline-1 receptor antagonist	Increase
Rilmenidine hemifumarate	Imidazoline receptor antagonist	Increase
2'5'dideoxyadenosine (2'5'ddA)	Adenylyl cyclase inhibitor	Increase
Forskolin	Adenylyl cyclase activator	Decrease
N^6, 2'-O-Dibutyryladenosine-cAMP	cAMP agonist	Decrease
8-CPT-2-Me-cAMP	Specific Epac activator	Decrease
6-Bnz-cAMP	Specific PKA activator	No effect
Calpastatin	Calpain inhibitor	Increase
Calpeptin	Calpain inhibitor	Increase
ALLM	Calpain inhibitor	Increase
PACAP 38 Ovine	Activates $G_{s\alpha}$	Decrease
NF449	Specific inhibitor of $G_{s\alpha}$	Increase
Thapsigargin	Ca^{2+}-ATPase inhibitor	Decrease
KT 5720	PKA inhibitor	Decrease
FPL61476	Ca^{2+} channel agonist	Decrease
Tolazamide	ATP-K^+ channel antagonist	Decrease
Quinine sulphate	ATP-K^+ channel antagonist	Decrease
Rolipram	Phosphodiesterase 4 inhibitor (increases cAMP)	Decrease

Supplementary Figure 1 continued

Supplementary Fig. 1. Schematic representation of calpain and caspase cleavage sites in huntingtin and the exon 1 fragment used in this study and table of screen hits and other compounds that modulate the clearance of aggregate-prone proteins.

a, Schematic representation of calpain and caspase cleavage sites in huntingtin and the exon 1 fragment used in this study. The approximate amino acid positions of the caspase and calpain cleavage sites in huntingtin[28] are indicated by arrows. The exon 1 fragment of huntingtin containing 74 polyQ repeats used in our study (as indicated in the figure) is N-terminal to the caspase and calpain cleavage sites and is thus unaffected of any cleavage events. See reference in Supplementary Information online.

b, List of screen hits and other compounds used in this study that modulate the clearance of aggregate-prone proteins. Table of screen hits and various compounds used in this study, their mode of action and their effect on the clearance of aggregate-prone proteins, such as mutant huntingtin fragment or mutant α-synucleins. Note that this is not a list of the entire library of compounds used in the screen.

Supplementary Figure 2

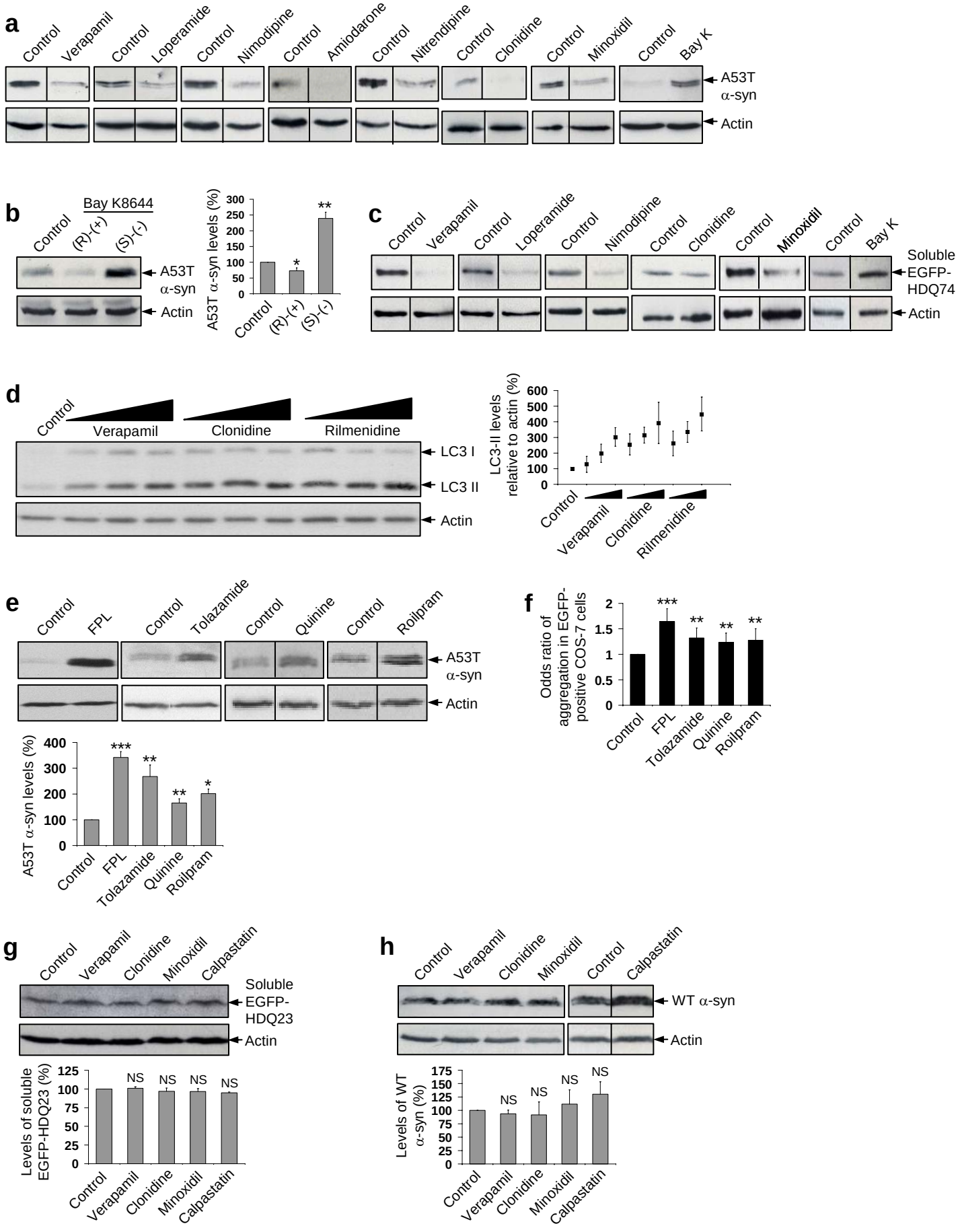

Supplementary Figure 2 continued

Supplementary Fig. 2. Screen hits that modulate the clearance of aggregate-prone proteins.

a, Screen hits that modulate the clearance of A53T α-synuclein. Stable inducible PC12 cells expressing A53T α-synuclein was induced with 1 μg/ml doxycycline for 48 h, then transgene was switched off (by removing doxycycline) for 24 h with or without verapamil, loperamide, nimodipine, nitrendipine, amiodarone, clonidine, minoxidil or (±)-Bay K8644 (all 1 μM). DMSO was control. A53T α-synuclein was detected with anti-HA antibody. Note that control clearance levels for a given substrate may vary from figure to figure, due to different exposures of blots, which aid illustration of agents that either increase or retard clearance. Densitometric analysis of A53T α-synuclein clearance relative to actin is shown in Fig. 1a.

b, Effect of Bay K8644 enantiomers on the clearance of A53T α-synuclein. Clearance of A53T α-synuclein in stable inducible PC12 cells as in Supplementary Fig. 2a, treated with DMSO (control), or with Bay K8644 enantiomers like 1 μM (R)-(+)-Bay K8644 (an L-type Ca^{2+} channel antagonist) or 1 μM (S)-(-)-Bay K8644 (an L-type Ca^{2+} channel agonist) for 24 h, was analysed by immunoblotting with anti-HA antibody and densitometric analysis relative to actin.

c, Screen hits that modulate the clearance of soluble EGFP-HDQ74. Stable inducible PC12 cells expressing EGFP-HDQ74 (mutant huntingtin) was induced with 1 μg/ml doxycycline for 8 h, then transgene was switched off (by removing doxycycline) for 96 h, with or without verapamil, loperamide, nimodipine, clonidine, minoxidil or (±)-Bay K8644 (all 1 μM). DMSO was control. Soluble EGFP-HDQ74 was detected with anti-EGFP antibody. Densitometric analysis of soluble EGFP-HDQ74 clearance relative to actin is shown in Fig. 1b.

d, Verapamil, clonidine and rilmenidine induce dose-dependent increases in autophagy. SK-N-SH cells treated with or without 0.33 μM, 1 μM or 3 μM verapamil, clonidine or rilmenidine for 24 h were assessed for endogenous LC3-II levels by immunoblotting with anti-LC3 antibody and densitometry analysis relative to actin.

e, Additional screen hits that retard the clearance of A53T α-synuclein. Clearance of A53T α-synuclein in stable inducible PC12 cell line as in Supplementary Fig. 2a, treated with DMSO (control), 10 μM FPL64176 (Ca^{2+} channel agonist), 10 μM tolazamide, 10 μM quinine sulphate (ATP-K^+ channel antagonists) or 10 μM rolipram (phosphodiesterase 4 inhibitor) for 24 h, was analysed by immunoblotting with anti-HA antibody and densitometry analysis relative to actin.

f, Additional screen hits that increase EGFP-HDQ74 aggregation. COS-7 cells were transfected with EGFP-HDQ74 for 4 h and treated with DMSO (control), 10 μM, 10 μM tolazamide, 10 μM quinine sulphate or 10 μM rolipram for 48 h post-transfection. The proportions of EGFP-positive cells with EGFP-HDQ74 aggregates were assessed and expressed as odds ratios.

g, h, Autophagy inducers do not affect the clearance of wild-type α-synuclein or huntingtin. Stable inducible PC12 cell lines expressing wild-type EGFP-tagged huntingtin exon 1 with 23 polyQ repeats (EGFP-HDQ23; wild-type huntingtin) (g) or wild-type HA-tagged α-synuclein (h) were induced with 1 μg/ml doxycycline for 8 h (g) or 48 h (h), then transgene was switched off (by removing doxycycline) for 72 h (g) or 24 h (h), with or without 1 μM verapamil, 1 μM clonidine, 1 μM minoxidil or 10 μM calpastatin. EGFP-HDQ23 (g) or wild-type HA-α-synuclein (h) levels were detected by immunoblotting with anti-EGFP (g) or anti-HA (h) antibodies and densitometry analysis relative to actin.

***, $p < 0.0001$; **, $p < 0.01$; *, $p < 0.05$; NS, Non-significant.

Supplementary Figure 3

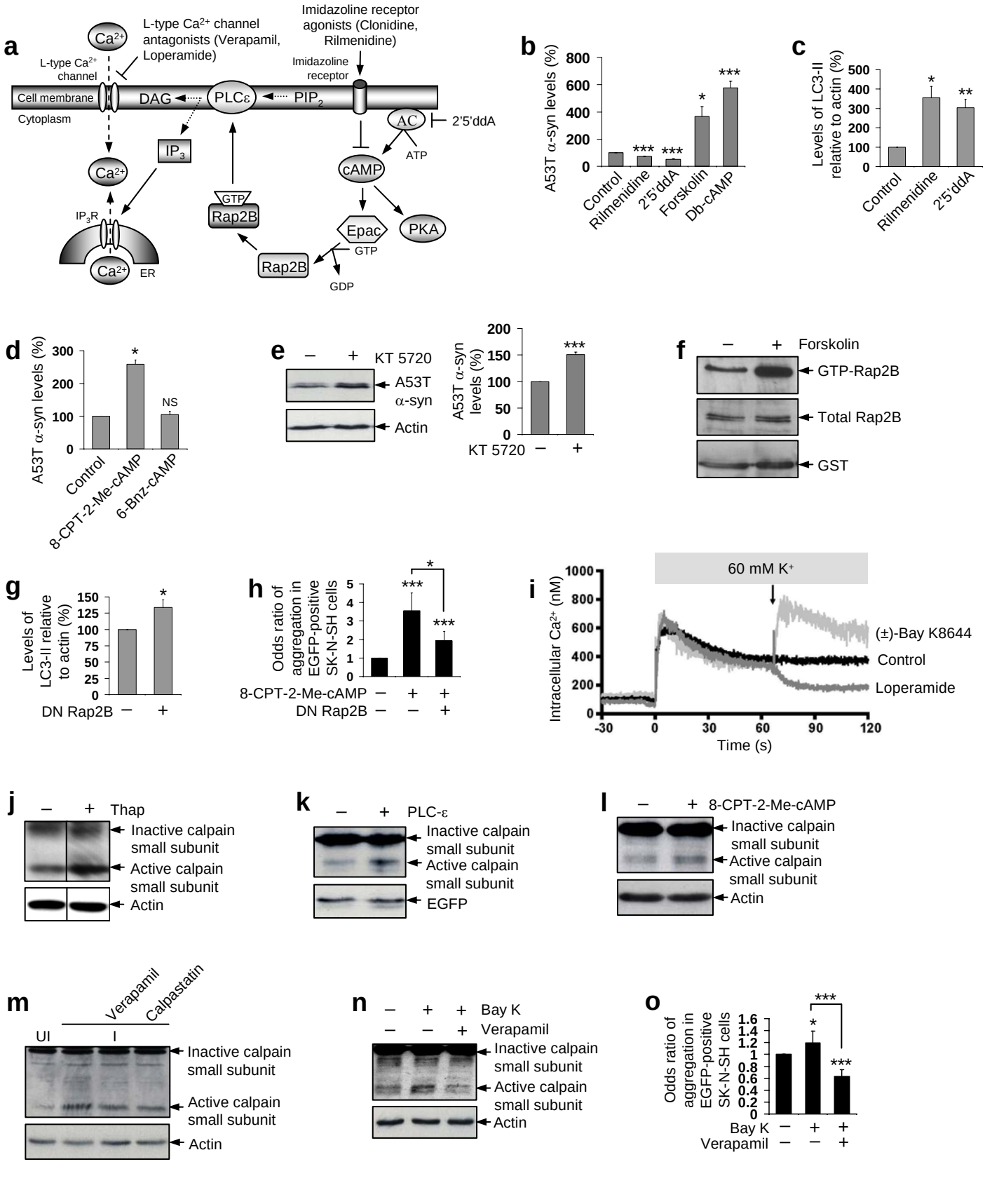

Supplementary Figure 3 continued

Supplementary Fig. 3. Modulators of cAMP and Ca^{2+} signalling and their effect on calpain activity and aggregate-prone proteins.

a, Schematic representation of autophagy regulators downstream of L-type Ca^{2+} channels and imidazoline receptors. Intracellular cAMP levels are increased by adenylyl cyclase (AC) activity, which is inhibited by 2'5'dideoxyadenosine (2'5'ddA). cAMP activates Epac which subsequently activates Rap2B, a small G-protein that activates PLC-ε resulting in the production of IP_3 and consequent Ca^{2+} release from the ER. Clonidine and rilmenidine bind to imidazoline-1 receptors on the cell membrane, which decrease cAMP levels and thereby inhibit the rise in intracellular Ca^{2+}. L-type Ca^{2+} channel antagonists like verapamil and loperamide also decrease intracellular Ca^{2+} by preventing extracellular Ca^{2+} entry. All the compounds shown in this pathway induce autophagy.

b, cAMP-lowering agents enhance the clearance of A53T α-synuclein, while those increasing cAMP levels retard the clearance. Densitometric analysis relative to actin of A53T α-synuclein clearance in stable inducible PC12 cells as in Fig. 2a, treated with DMSO (control) or with 1 μM rilmenidine, 500 μM 2'5'ddA, 24 μM forskolin or 1 mM db-cAMP for 24 h.

c, Compounds decreasing cAMP levels induce autophagy. Densitometric analysis of endogenous LC3-II levels relative to actin in PC12 cells as in Fig. 2c, treated with DMSO (control) or with 1 μM rilmenidine or 500 μM 2'5'ddA for 24 h.

d, Epac-specific, but not PKA-specific, cAMP analogue inhibits the clearance of A53T α-synuclein. Densitometric analysis relative to actin of A53T α-synuclein clearance in stable inducible PC12 cells as in Fig. 2d, treated with DMSO (control) or with 1 or 10 μM 8-CPT-2Me-cAMP or 6-Bnz-cAMP for 24 h.

e, Effect of protein kinase A inhibitor on the clearance of A53T α-synuclein. A53T α-synuclein clearance in stable inducible PC12 cells, treated with DMSO (control) or 1 μM KT5720 for 24 h, was analysed by immunoblotting with anti-HA antibody and densitometry analysis relative to actin.

f, Forskolin activates Rap2B. Activation of the small GTPase Rap2B in PC12 cells. PC12 cells were treated with DMSO (control) or 24 μM forskolin for 30 min. Following lysis, GTP-bound active Rap2B was precipitated using immobilised GST-RalGDS-RBD and identified by immunoblotting with anti-Rap2B antibody.

g, Dominant negative Rap2B induces autophagy. Densitometric analysis of endogenous LC3-II levels relative to actin in COS-7 cells as in Fig. 2g, transfected with pcDNA3.1 (empty vector) or with dominant negative S17N Rap2B (DN Rap2B), were analysed at 24 h post-transfection.

h, Dominant negative Rap2B abolishes the effects of Epac-specific cAMP analogue on mutant huntingtin aggregation. SK-N-SH cells transfected with EGFP-HDQ74 and empty vector (pcDNA3.1) or dominant-negative S17N Rap2B (DN Rap2B) (1:3 ratio) for 4 h were treated with or without 10 μM 8-CPT-2Me-cAMP. The proportions of EGFP-positive cells with aggregates were assessed at 48 h.

i, L-type Ca^{2+} channel antagonists decrease, whereas L-type Ca^{2+} channel agonists increase intracytosolic Ca^{2+} concentrations. Intracellular Ca^{2+} measurements of Fura2-loaded PC12 cells were determined during activation of voltage-gated Ca^{2+} channels by membrane depolarisation achieved by addition of extracellular KCl (60 mM) and subsequent addition (arrow) of loperamide (1 μM; dark grey), (±)-Bay K8644 (1 μM; light grey) or vehicle alone (control; black). Traces shown are representative of at least 3 separate experiments. Similar reductions in intracellular Ca^{2+} were observed following addition of verapamil and nimodipine (data not shown).

j, Thapsigargin activates calpains. Calpains were activated with the endoplasmic reticulum (ER) Ca^{2+}/Mg^{2+} ATPase inhibitor, thapsigargin, which increases intracellular Ca^{2+} levels. COS-7 cells were treated with DMSO (control) or 2.5 μM thapsigargin for 30 min, and calpain activation was analysed by immunoblotting with antibody against calpain small subunit.

k, Overexpression of PLC-ε activates calpain. COS-7 cells transfected with pcDNA3.1 (empty vector) or wild type PLC-ε for 4 h were assessed for levels of calpain activity at 48 h post-transfection by immunoblotting with anti-calpain small subunit antibody.

l, Epac-specific cAMP analogue activates calpain. COS-7 cells treated with or without 10 μM 8-CPT-2-Me-cAMP for 24 h were assessed for levels of calpain activity by immunoblotting with anti-calpain small subunit antibody.

m, Verapamil and calpastatin reduce the increased calpain activation in mutant huntingtin cell line. PC12 stable inducible cells expressing EGFP-HDQ74 were pre-treated with or without 1 μM verapamil or 10 μM calpastatin for 30 min. Cells were then left uninduced (UI) or induced (I) with 1 μg/ml doxycycline for 8 h, followed by a further treatment with or without 1 μM verapamil or 10 μM calpastatin for 24 h. Calpain activity was assessed by the levels of active calpain small subunit by immunoblotting with anti-calpain small subunit antibody.

n, Verapamil reduces calpain activity. SK-N-SH cells were treated with DMSO (control) or 1 μM (±)-Bay K8644 for 4 h in presence or absence of 1 μM verapamil. Calpain activation was assessed by the levels of active calpain small subunit, which was detected with anti-calpain small subunit antibody. Cells were pre-treated with verapamil for 15 min prior to (±)-Bay K8644 treatment.

o, Verapamil reduces (±)-Bay K8644-induced increase in EGFP-HDQ74 aggregation. The proportions of EGFP-positive SK-N-SH cells with EGFP-HDQ74 aggregates as in Fig. 1c, treated with DMSO (control) or 1 μM (±)-Bay K8644 in presence or absence of 1 μM verapamil for 48 h post-transfection, were assessed.

***, $p < 0.001$; **, $p < 0.01$; *, $p < 0.05$; NS, Non-significant.

Supplementary Figure 4

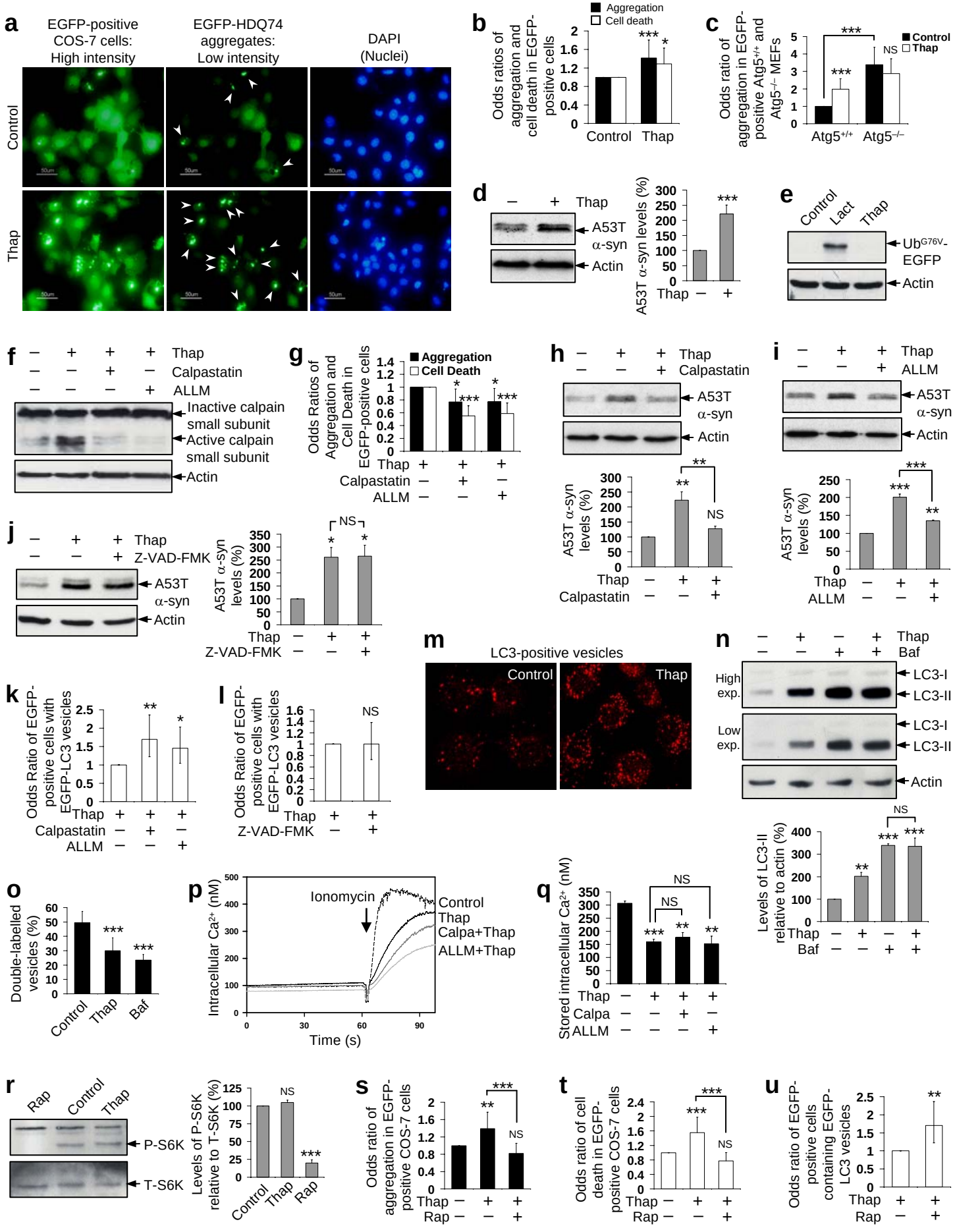

Supplementary Figure 4 continued

Supplementary Fig. 4. The effects of thapsigargin on the clearance of mutant proteins are rescued by calpain inhibitors and thapsigargin inhibits autophagy by blocking autophagosome-lysosome fusion.

a, b, Thapsigargin increases EGFP-HDQ74 aggregation and cell death. COS-7 cells were transfected with EGFP-HDQ74 for 4 h and then treated with DMSO (control) or 2.5 μM thapsigargin (thap) for last 24 h of 48 h post-transfection period. Fluorescent microscopy images were taken in high (left panel) and low intensity (middle panel) to denote the number EGFP-positive transfected cells and aggregates (indicated by arrows) respectively (a). Nuclei are stained with DAPI (right panel). Bar, 50 μM (a). The effects of thapsigargin on EGFP-HDQ74 aggregation and cell death at 48 h post-transfection were expressed as odds ratio (b).

c, The effect of thapsigargin on EGFP-HDQ74 aggregation is autophagy-dependent. The proportions of EGFP-positive cells with EGFP-HDQ74 aggregates in wild type (*Atg5*$^{+/+}$) and knockout (*Atg5*$^{-/-}$) Atg5 mouse embryonic fibroblasts (MEFs), transfected with EGFP-HDQ74 for 4 h and then treated for next 48 h with or without 2.5 μM thapsigargin, were expressed as odds ratio. Thapsigargin increased aggregates in *Atg5*$^{+/+}$, but not in *Atg5*$^{-/-}$, suggesting its effect was autophagy-dependent.

d, Thapsigargin retards clearance of A53T α-synuclein. A53T α-synuclein clearance in stable inducible PC12 cells, treated with DMSO (control) or 2.5 μM thapsigargin for 24 h, was analysed by immunoblotting with anti-HA antibody and densitometry analysis relative to actin.

e, The effects of thapsigargin on the clearance of aggregate-prone proteins are proteasome-independent. HeLa cells stably expressing Ub^{G76V}-EGFP reporter, treated with or without 10 μM lactacystin (lact) or 2.5 μM thapsigargin for 24 h, were analysed for proteasome activity by immunoblotting with anti-EGFP antibody.

f, Activation of calpains by thapsigargin can be abolished by calpain inhibitors. COS-7 cells were treated with DMSO (control) or 2.5 μM thapsigargin in presence or absence of 10 μM calpastatin or 50 μM ALLM for 30 min. Calpain activation was analysed with anti-calpain small subunit antibody. Cells were pre-treated with calpastatin or ALLM for 15 min before adding thapsigargin, and such pre-treatment was done in the following experiments in Supplementary Figs. 4f–i, k online.

g, The effects of thapsigargin on EGFP-HDQ74 aggregation and toxicity can be rescued by calpain inhibitors. The proportions of EGFP-positive cells with EGFP-HDQ74 aggregates or cell death in COS-7 cells as in Fig. 1c, treated with 2.5 μM thapsigargin in presence or absence of 10 μM calpastatin or 50 μM ALLM for the last 24 h of the 48 h post-transfection period.

h–j, The effects of thapsigargin on A53T α-synuclein clearance can be abolished by calpain inhibitors but not by caspase inhibitors. A53T α-synuclein clearance in stable inducible PC12 cells as in Supplementary Fig. 4d online, treated with DMSO (control) or 2.5 μM thapsigargin in presence or absence of 10 μM calpastatin (h), 50 μM ALLM (i) or 20 μM caspase inhibitor I (Z-VAD-FMK) (j) for 24 h, was analysed by immunoblotting with anti-HA antibody and densitometry analysis relative to actin.

k, l, Calpain inhibitors rescue the effects of thapsigargin on autophagy. COS-7 cells were transfected with EGFP-LC3 construct for 4 h and treated with 2.5 μM thapsigargin with or without 10 μM calpastatin or 50 μM ALLM (k), or 20 mM caspase inhibitor I (Z-VAD-FMK) (l) for 2 h. The proportions of EGFP-positive cells with >5 EGFP-LC3 vesicles were assessed.

m, Thapsigargin increases LC3-positive vesicles. COS-7 cells treated with DMSO (control) or 2.5 μM thapsigargin for 2 h, were analysed by immunofluorescence with anti-LC3 antibody.

n, Thapsigargin is not an inducer of autophagy since it does not increase LC3-II levels in bafilomycin A1-treated cells. COS-7 cells were treated for 4 h with or without 400 nM bafilomycin A1 (baf), or with 400 nM bafilomycin A1 in presence or absence of 2.5 μM thapsigargin. Cells were pre-treated with DMSO (control) or thapsigargin for 24 h before adding bafilomycin A1. LC3-II levels were measured by immunoblotting with anti-LC3 antibody and densitometry analysis of LC3-II relative to actin.

o, Thapsigargin inhibits autophagosome-lysosome fusion. Normal rat kidney (NRK) cells were transiently transfected with LC3 tagged with the red fluorescent protein mCherry and the late endosomal/lysosomal membrane protein lgp120 tagged with GFP. They were then treated with DMSO (control), 2.5 μM thapsigargin or 400 nM bafilomycin A1 for 24 h. Similar to bafilomycin A1 (negative control), thapsigargin led to a clear decrease in colocalisation and therefore autophagosome-lysosome fusion (2 experiments, 20 cells per treatment per experiment, two-tailed *t*-test: *p* (DMSO, thap) = $9x10^{-9}$; *p* (DMSO, baf) = $1x10^{-13}$.

p, q, Calpain inhibitors do not affect intracellular stored Ca^{2+} in the presence of thapsigargin. Stored intracellular Ca^{2+} was determined by addition of 10 μM ionomycin (arrow) to Fura2-loaded COS-7 cells resuspended in nominally Ca^{2+}-free saline. Representative traces are shown following 24 h treatment of cells with DMSO control (dashed), 2.5 μM thapsigargin (black), 2.5 μM thapsigargin and 10 μM calpastatin (dark grey) and 2.5 μM thapsigargin and 50 μM ALLM (light grey) (p). Peak ionomycin-releasable Ca^{2+} (mean ± s.d., n = 3) are shown under the same conditions (q).

r, Effects of thapsigargin are mTOR-independent. COS-7 cells treated with DMSO (control), 2.5 μM thapsigargin or 0.2 μM rapamycin (rap) for 24 h, were analysed for mTOR activity by immunoblotting for levels phospho-S6K and densitometry analysis of phospho-S6K relative to total S6K. Rapamycin was used as a positive control to assess mTOR inhibition. Likewise, verapamil, loperamide, nimodipine, clonidine and minoxidil had no effect on mTOR signaling (data not shown).

s, t, Thapsigargin-induced EGFP-HDQ74 aggregation/toxicity can be abrogated by rapamycin. The percentage of EGFP-HDQ74-positive cells with aggregates and cell death in COS-7 cells, treated with 2.5 μM thapsigargin with or without 0.2 μM rapamycin for the last 24 h of the 48 h post-transfection period, was expressed as odds ratio. Rapamycin treatment was started 15 min prior to addition of thapsigargin.

u, Rapamycin rescues the effects of thapsigargin on autophagy. COS-7 cells were transfected with EGFP-LC3 construct for 4 h and treated with 2.5 μM thapsigargin with or without 0.2 μM rapamycin for 2 h. The proportions of EGFP-positive cells with >5 EGFP-LC3 vesicles were assessed. Rapamycin treatment was started 15 min prior to addition of thapsigargin.

*, $p < 0.05$; **, $p < 0.01$; ***, $p < 0.001$; NS, Non-significant.

Supplementary Figure 5

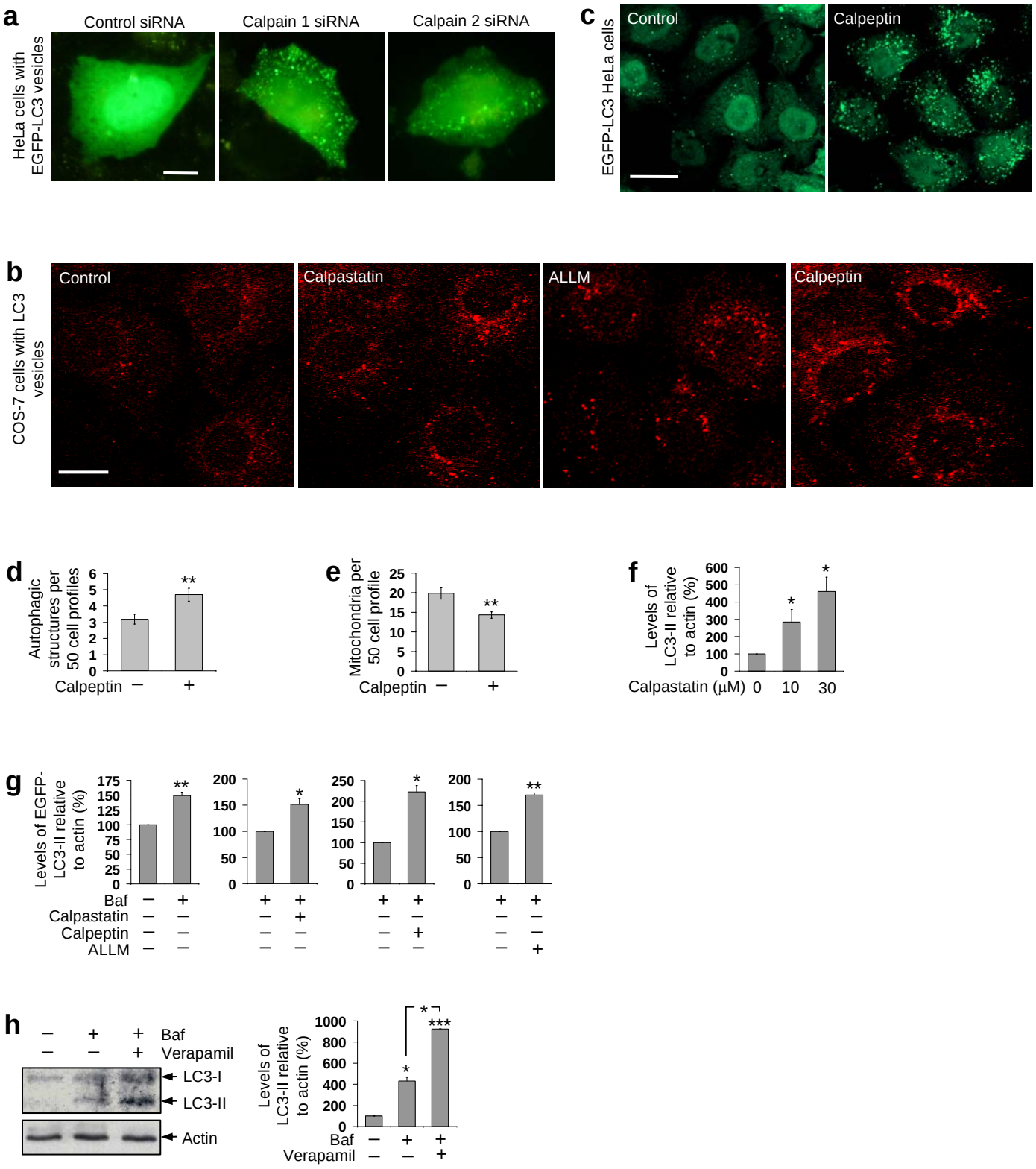

Supplementary Figure 5 continued

Supplementary Fig. 5. Calpain inhibition induces autophagy.

a, Knockdown of calpain 1 or 2 increases EGFP-LC3 vesicles. HeLa cells were transfected with si*GLO* (control siRNA) with or without calpain 1 siRNA or calpain 2 siRNA (1:3 ratio) for 96 h, followed by transfection with EGFP-LC3 construct for 4 h. Cells were fixed after a further 2 h and analysed by fluorescence microscopy to identify EGFP-positive cells with EGFP-LC3 vesicles that are also si*GLO*-positive. Bar, 50 μm. The proportions of EGFP- and si*GLO*-positive cells with >5 EGFP-LC3 vesicles were counted and shown in Fig. 5b.

b, Calpain inhibitors increases LC3-positive vesicles. COS-7 cells treated with or without 10 μM calpastatin, 50 μM ALLM or 50 μM calpeptin for 24 h, were analysed by immunofluorescence with anti-LC3 antibody. Bar, 20 μm.

c, Calpain inhibitors increases EGFP-LC3 vesicles in stable HeLa cells. HeLa cells stably expressing EGFP-LC3 were treated with or without 50 μM calpeptin for 24 h. Confocal microscopy images show cells containing EGFP-positive autophagic vesicles. Bar, 100 μm. Similar trends were seen with calpastatin and ALLM (data not shown).

d, e, Calpeptin increases autophagosome-like structures and reduces mitochondria. COS-7 cells were treated with DMSO (control) or 50 μM calpeptin for 24 h, fixed and assessed by electron microscopy (EM) for the number of early and late autophagosome-like structures (d) and mitochondria (e) per 50 cell profiles. EM analysis of autophagosomes was performed using criteria as described[21]. The data was analysed using Student's *t*-test and the error bar denotes standard error of the mean. See reference in Supplementary Information online.

f, Calpastatin induces autophagy in a dose-dependent fashion. Densitometric analysis of endogenous LC3-II levels in SK-N-SH cells as in Fig. 5c, treated with or without 10 mM or 30 mM calpastatin for 24 h.

g, Calpain inhibitors increase autophagic flux. Densitometry analysis of EGFP-LC3-II levels relative to actin of the immunoblot in Fig. 5d. In the left hand panel we show the effect of bafilomycin A1 (baf) on EGFP-LC3-II levels in cells not exposed to calpain inhibitors. For the other panels, we have fixed the EGFP-LC3-II levels in bafilomycin A1-treated cells not exposed to calpain inhibitors at 100% to facilitate comparisons – note that the data from different calpain inhibitors are from different blots, hence the band intensities in cells not exposed to calpain inhibitors cannot be directly compared.

h, Verapamil increases autophagic flux. Stable PC12 cells differentiated with 100 ng/ml NGF for 5 days were treated with or without 400 nM bafilomycin A1 (baf) in presence or absence of 1 μM verapamil for 4 h. Verapamil pre-treatment was done for 24 h before bafilomycin A1 addition. LC3-II levels were detected by immunoblotting with anti-LC3 antibody and densitometry analysis relative to actin.

Supplementary Figure 6

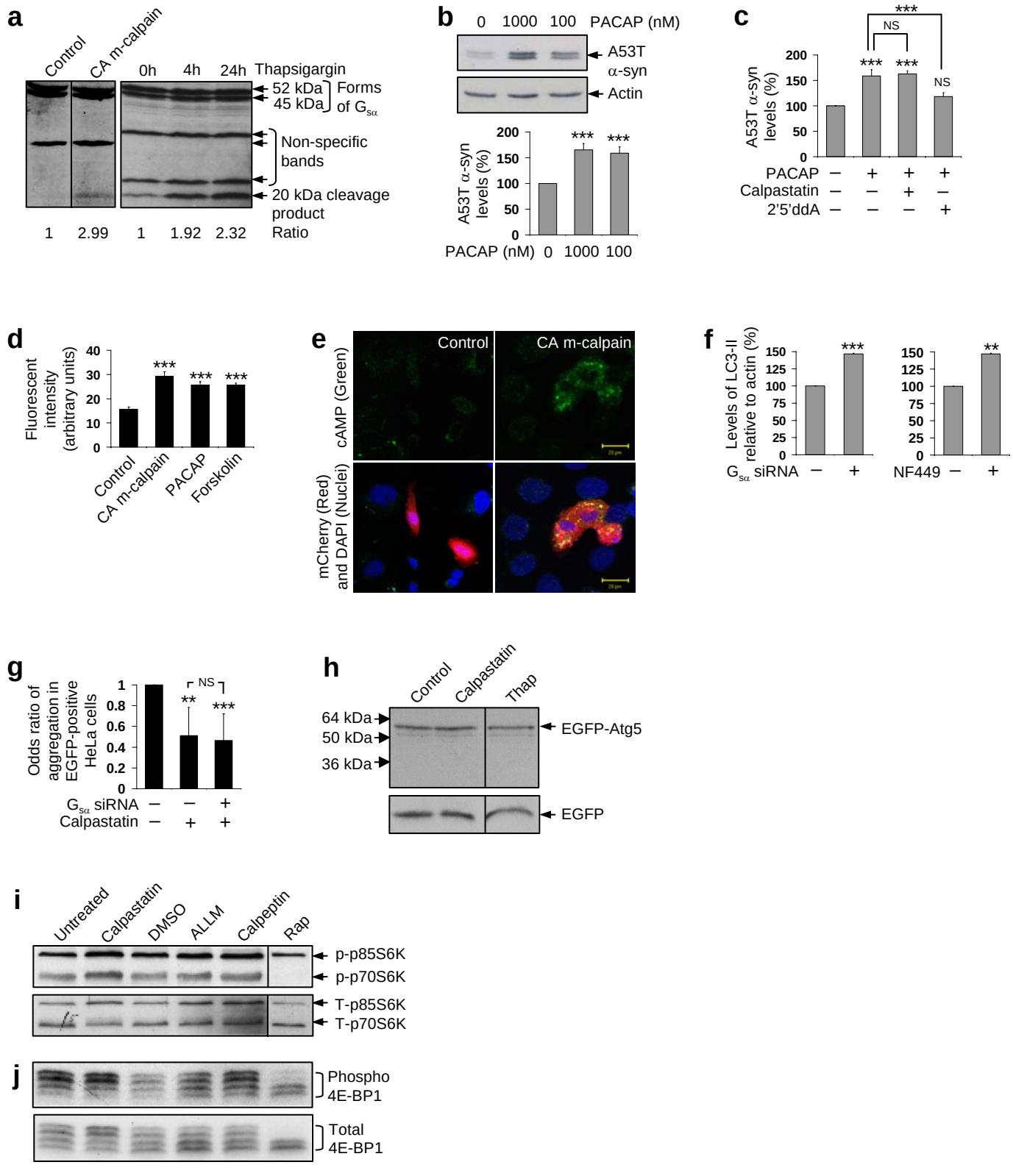

Supplementary Figure 6 continued

Supplementary Fig. 6. Calpain regulates autophagy by $G_{s\alpha}$ cleavage and cAMP-Epac pathway independently of mTOR.
a, Calpain activation cleaves and activates $G_{s\alpha}$. COS-7 cells, either treated with DMSO (control) or 2.5 μM thapsigargin for 24 h, or transfected with either pcDNA3.1 (empty vector) or constitutively active (CA) S50E m-calpain for 4 h and left for 48 h, were analysed for $G_{s\alpha}$ cleavage by immunoblotting with anti-$G_{s\alpha}$ antibody. Ratio of cleaved/uncleaved $G_{s\alpha}$ as a function of the control ratio (taken as 1) is shown. Note that the amount cleaved in control conditions in two different experiments is likely to be a function of the different control conditions (pcDNA3.1 transfection for CA m-calpain and DMSO for thapsigargin) and different gel exposures. Despite almost identical levels of the two full-length forms of $G_{s\alpha}$ (52 and 45 kDa) by scanning, the 20 kDa cleavage product was evident when calpains were induced. Similar trends are seen with wild-type calpain (data not shown), consistent with published data[29]. This cleavage product is constitutively active, and even low levels are biologically significant. See reference in Supplementary Information online.
b, $G_{s\alpha}$ activator PACAP inhibits the clearance of A53T α-synuclein. A53T α-synuclein clearance in stable PC12 cells, treated with or without 1 μM or 100 nM pituitary adenylyl-cyclase activating polypeptide (PACAP) for 24 h, was analysed by immunoblotting with anti-HA antibody and densitometry analysis relative to actin.
c, Adenylyl cyclase inhibitor, but not calpain inhibitor, abolishes the inhibitory effect of PACAP on A53T α-synuclein clearance. Densitometric analysis of A53T α-synuclein clearance relative to actin in stable inducible PC12 cells as in Fig. 6a, treated with or without 100 nM PACAP in the presence or absence of 10 μM calpastatin or 500 μM 2'5'ddA for 24 h.
d, e, Activation of calpain, $G_{s\alpha}$ or adenylyl cyclase increases cAMP levels. COS-7 cells were co-transfected with mCherry (red, transfection control) and either pcDNA3.1 (control) or constitutive active (CA) m-calpain (1:3 ratio) for 4 h. The mCherry and pcDNA3.1 transfected cells were treated with or without 24 μM forskolin or 1 μM PACAP for 24 h. Cells were subjected to immunocytochemistry with rabbit anti-cAMP antibody and goat anti-rabbit Alexa 488 green secondary antibody. Green fluorescence intensity (arbitrary units) was measured by confocal microscopy in 20 mCherry (red)-positive cells per slide in triplicate samples. Unpaired *t*-tests were performed on the means from each triplicate samples and the error bars denote standard error of the mean (d). Confocal microscope images show cAMP fluorescence (green) in pcDNA3.1 or CA m-calpain transfected cells (red, mCherry) (e). cAMP fluorescence was higher in CA m-calpain-transfected cells (red). Bar, 20 μm (e).
f, Inhibition of $G_{s\alpha}$ induces autophagy. Densitometric analysis of endogenous LC3-II levels relative to actin as in Figs. 6e, f, where $G_{s\alpha}$ siRNA (Fig. 6e) or $G_{s\alpha}$ inhibitor NF449 (Fig. 6f) increases LC3-II levels.
g, Knockdown of $G_{s\alpha}$ and calpastatin do not have additive effect on EGFP-HDQ74 aggregation. HeLa cells were transfected with control siRNA or *SMART*pool siRNA against $G_{s\alpha}$ together with EGFP-HDQ74 and treated with or without 10 μM calpastatin for 72 h. The proportion of EGFP-positive cells with EGFP-HDQ74 aggregates were assessed and expressed as odds ratio.
h, Modulators of calpain activity do not affect Atg5 levels or cleavage. COS-7 cells, transfected with EGFP-Atg5 and EGFP (transfection control) in a 3:1 ratio for 4 h and then treated with or without 10 μM calpastatin or 2.5 μM thapsigargin for 48 h, were analysed by immunoblotting with anti-EGFP antibody.
i, j, Calpain inhibitors do not inhibit mTOR activity. COS-7 cells treated with or without 10 μM calpastatin, 50 μM ALLM, 50 μM calpeptin, 0.2 μM rapamycin (rap) or DMSO (control for ALLM, calpeptin and rapamycin) for 24 h, were analysed for mTOR activity by immunoblotting for levels phospho-p70S6K (i) and phospho-4E-BP1 (j). Rapamycin was used as a positive control to assess mTOR inhibition.
**, $p < 0.01$; ***, $p < 0.0001$; NS, Non-significant.

Supplementary Figure 7

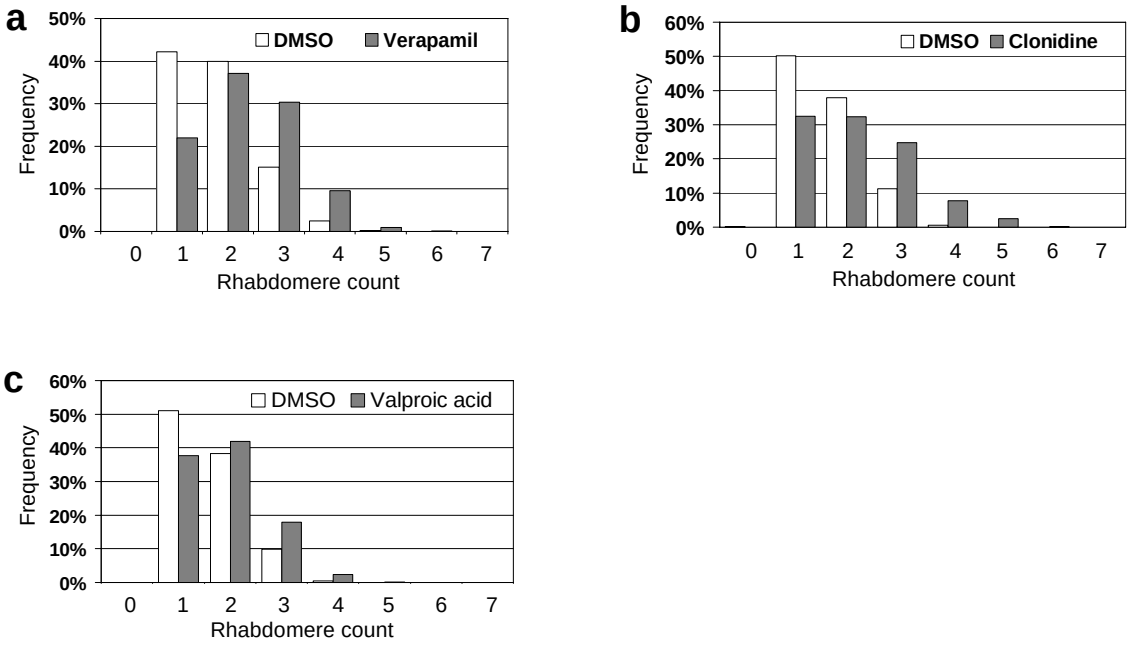

Supplementary Fig. 7. Verapamil, clonidine and valproic acid rescue neurodegeneration in a *Drosophila* model of Huntington's disease.

a–c, The compound eye of Drosophila consists of many ommatidia, each composed of eight photoreceptor neurons with light-gathering parts called rhabdomeres, seven of which can be visualised under a light microscope using the pseudopupil technique[24]. Neurodegeneration in the HD flies is progressive and is associated with a decrease in the number of visible rhabdomeres in each ommatidium with time[22]. Flies treated with either 1.87 mM verapamil hydrochloride, 500 μM clonidine, or 500 μM valproic acid show a shift in the distribution of the number of rhabdomeres compared to flies treated with DMSO (control) alone (2 days after eclosion). Rhabdomere counts from three or more independent experiments are included. At least 930 (a, b) or 1350 (c) ommatidia were scored under each condition. Verapamil also protected at 1.25 mM and 2.5 mM (data not shown). Mann-Whitney values for all experiments $p<0.0001$ (all treatments). When means of individual experiments were compared by Student's *t*-test, $p<0.05$ in all cases. See references in Supplementary Information online.

Supplementary Figure 8

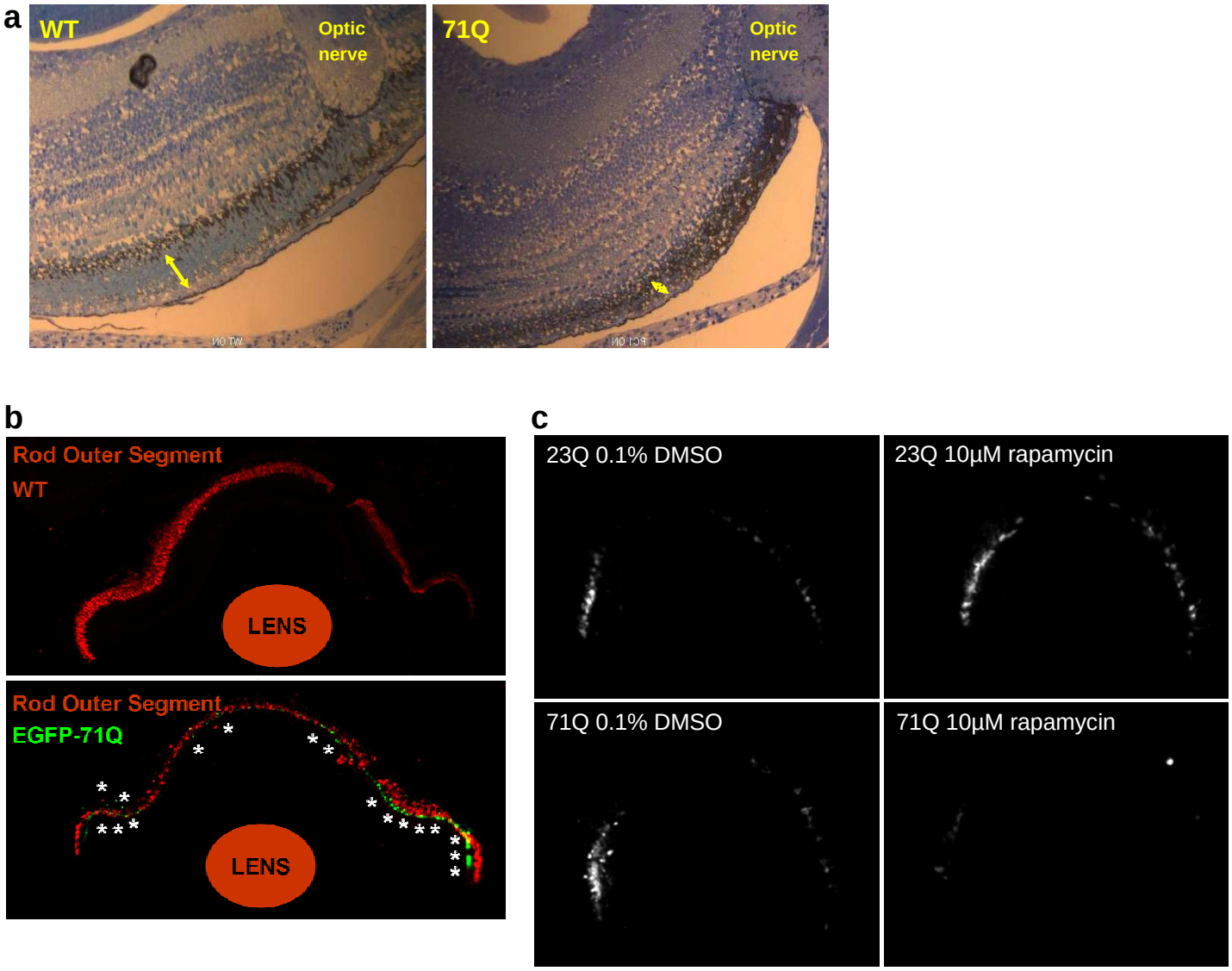

Supplementary Fig. 8. PolyQ-induced degeneration of rod photoreceptors in HD zebrafish model.

a, Loss of rod outer segments in HD zebrafish model. Methylene blue stained sections on adult fish. In wild-type retina, the retinal pigment epithelium interdigitates with rod outer segments following a period of light adaptation. Rod outer segments are marked by the double arrowhead. In the EGFP-HDQ71, there was a loss of rod outer segments in the region marked with the double arrowhead.

b, Reduced rhodopsin expression in HD zebrafish model. Adult zebrafish were sectioned as described and probed with 1:200 Zpr3 (red). Reduced rhodopsin expression can be seen in the EGFP-HDQ71 line.

c, Rapamycin reduces mutant huntingtin aggregates in HD zebrafish model. In the EGFP-HDQ23 line sectioned at 9 d.p.f., no aggregates formed and no effect was observed by 10 µM rapamycin treatment. In the EGFP-HDQ71 line, aggregates were apparent in vehicle (DMSO) treated samples and both aggregate burden and diffuse EGFP-HDQ71 was noticeably reduced by 10 µM rapamycin. This is entirely consistent with our previous data in cell models showing that wild-type mutant huntingtin fragments are very poor autophagy substrates, while both soluble and aggregated forms of mutant huntingtin are cleared efficiently after autophagy induction[15,30]. It is likely that aggregates are cleared because autophagy is removing aggregate precursors (i.e., soluble monomeric/oligomeric species), rather than the aggregates themselves, which are not membrane-bound. For detailed discussion, see review[31]. See references in Supplementary Information online.